# Comparative analysis of dynamic balance descriptors in humanoids and humans during perturbed bipedal locomotion and fall

Sirikorn Chalanunt, Ariane Lallès, Arnaud Demont, Mehdi Benallegue, Bruno Watier, Hélène Pillet

▶ **To cite this version:**

Sirikorn Chalanunt, Ariane Lallès, Arnaud Demont, Mehdi Benallegue, Bruno Watier, et al.. Comparative analysis of dynamic balance descriptors in humanoids and humans during perturbed bipedal locomotion and fall. International Conference on Humanoid Robots, IEEE, Sep 2025, Seoul, South Korea. pp.1-8, ⟨10.1109/Humanoids65713.2025.11203160⟩. ⟨hal-05407361⟩

**HAL Id: hal-05407361**

**https://hal.science/hal-05407361v1**

Submitted on 9 Dec 2025

**HAL** is a multi-disciplinary open access archive for the deposit and dissemination of scientific research documents, whether they are published or not. The documents may come from teaching and research institutions in France or abroad, or from public or private research centers.

L'archive ouverte pluridisciplinaire **HAL**, est destinée au dépôt et à la diffusion de documents scientifiques de niveau recherche, publiés ou non, émanant des établissements d'enseignement et de recherche français ou étrangers, des laboratoires publics ou privés.

HAL Authorization

# Comparative Analysis of Dynamic Balance Descriptors in Humanoids and Humans during Perturbed Bipedal Locomotion and Fall

Sirikorn Chalanunt[1,2,3], Ariane Lallès[3,5], Arnaud Demont[1,4], Mehdi Benallegue[1], Bruno Watier[1,5], and Hélène Pillet[3]

***Abstract*— This study identifies a robust parameter for quantifying instability in general biped systems by comparing three mechanical stability descriptors: the distance between the center of mass to the minimal moment axis ($d_{\text{CoM-MMA}}$), the margin of stability (MoS), and whole-body angular momentum (WBAM) in both humans and humanoid biped robots. We analyzed these metrics during normal and perturbed walking, including robot falls, a dynamic whose observation is limited in human trials due to safety concerns. Our comparative analyses demonstrate that $d_{\text{CoM-MMA}}$ is more predictive of different levels of instability and shows a clearer distinction between fall and non-fall states, compared to MoS and WBAM. These findings were consistent for both humans and biped robots, regardless of gait variability or the type and intensity of the perturbation methods. These qualities highlight its potential use in unified stability analysis in both fields, offering insights that can inform the design of exoskeletons, fall monitoring systems, and other gait-assistive devices for aging populations.**

***Index Terms*— bipedal locomotion, perturbation, fall, human biomechanics, biped robot.**

## I. INTRODUCTION

The control of balance during bipedal locomotion represents a very complex task whether in humans or biped robots. Identifying a mechanical descriptor able to predict the evolution of balance would be useful for both robot motion generation and monitoring in clinical fellow up of people with impaired locomotion. These mutual benefits highlight the importance of developing robust stability descriptors that enable precise stability quantification across domains. In this paper, we analyze dynamic balance descriptors applicable for both humans and biped robots, i.e., robots with exactly two lower limbs capable of independent stance and swing phases, regardless of their anthropomorphism. While numerous stability measures have been proposed [1], [2], their effectiveness in capturing dynamic balance under varying perturbations and domains remains a subject of ongoing research.

The early and widely used approach to quantify balance was a by-product of the concept of the Linear Inverted Pendulum Model (LIPM). LIPM is foundational for analyzing and controlling legged systems, assuming low angular momentum and using the Zero Moment Point (ZMP) to describe dynamics [3], [4]. To account for system dynamics and additional disturbances, a Model Predictive Control (MPC) approach was introduced to reduce ZMP tracking errors and smoothen center of mass (CoM) trajectories [5], [6]. A more general concept of the Divergent Component of Motion (DCM), derived from the mode analysis of linearized dynamical systems, provides a powerful way to analyze and control balance. It was initially conceptualized in 2D [7], the later extended to 3D [8]. The 2D ground projection of DCM is equivalent to the Capture Point (CP), which represents the exact location where a robot must place its foot to come to a complete stop [9], [10]. In biomechanics, a parallel concept was developed to describe stability in human static poses and normal gait. Hof introduced the Extrapolated Center of Mass (XCoM) which is equivalent to the CP to define the Margin of Stability (MoS) as the distance from the XCoM to the boundary of the base of support (BoS) [11].

Extensions went beyond the LIPM, such as allowing angular momentum variations [12], [13]. Angular momentum-based strategies also predict foot placement using contact point dynamics [14]. Whole-body angular momentum (WBAM) is also widely studied in biomechanics for its role in predicting instability and falls [15], [16], [17], [18]. To address ZMP limitations in multi-contact scenarios, the descriptor $\boldsymbol{d}_{\text{CoM-MMA}}$— distance from the CoM to the minimal moment axis (MMA)—was developed [2]. MMA corresponds to the line where the moment of the external wrench is minimal and aligns with the external resultant force [19], [2], [20]. In biomechanics, $\boldsymbol{d}_{\text{CoM-MMA}}$ reflects instability differences across groups, walking strategies, conditions, and age differences [20], [21].

The approach of using whole body dynamical system analysis to describe the stability of bipeds had also been studied through the use of maximum Lyapunov exponents and Floquet multipliers [22]. While these parameters can represent a certain degree of system stability [23], [24], their

* This work includes results obtained from the project "Programs for Bridging the Gap between R&D and the Ideal Society (Society 5.0) and Generating Economic and Social Value (BRIDGE)/Practical Global Research in the AI × Robotics Services", implemented by the Cabinet Office, Government of Japan.

* This work was supported in part by the National Research Agency (ANR) under project ANR-22-CE19-0003-01 and the Fondation de l'Avenir (grant number AP-RM-20-001).

* This work involved human subjects in its research. Approval of all ethical and experimental procedures and protocols was granted under the ethical agreement number: RCB 2020-A01357-32.

[1] S. Chalanunt, A. Demont, M. Benallegue, B. Watier are with CNRS-AIST JRL (Joint Robotics Laboratory), IRL, National Institute of Advanced Industrial Science and Technology (AIST), Tsukuba, Japan.

[2] S. Chalanunt is also with ESPCI Paris, PSL University, Paris, France.

[3] A. Lalles, H. Pillet and S. Chalanunt are also with Arts et Métiers Institute of Technology, Institut de Biomécanique Humaine Georges Charpak (IBHGC), Paris, France.

[4] A. Demont is also with Université Paris-Saclay, Gif-sur-Yvette, France, and Laboratoire d'Ingénierie des Systèmes de Versailles (LISV), France.

[5] A. Lalles and B. Watier are also with Laboratoire d'Analyses et d'Architecture des Systèmes (LAAS-CNRS), Toulouse, France.

implementation in real-world setting are challenging and subjected to limitations [25], especially in distinguishing fall-prone gaits [26]. Due to the problem of model complexities in human and biped robots, noisy sensors, and non-periodic non-stationary nature of real-world gaits [27], [25], [28], these parameters are not suitable for the scope of this study.

A universal balance metric for humans and bipedal robots would advance both fields. Although ethical restrictions limit human studies, robots can be tested in extreme conditions; this collaboration could offer biomechanists insights into extreme conditions and guide roboticists in refining bioinspired balance control, especially since previous comparative studies have not included newer metrics such as $\boldsymbol{d}_{\text{CoM-MMA}}$ [1], [29], [30].

In this paper we propose the following contributions

- Demonstrate that $\boldsymbol{d}_{\text{CoM-MMA}}$ is a sensitive metric for detecting imbalance common to both humans and biped robots, regardless of the perturbation level or method, while effectively representing the varying levels of induced instability.
- Study the correlations and differences in $\boldsymbol{d}_{\text{CoM-MMA}}$ between humans and biped robots, providing insights into the transferability of stability analysis across these entities.
- Offer a comparative performance analysis of $\boldsymbol{d}_{\text{CoM-MMA}}$ against other widely used criteria in biomechanics and robotics, such as the margin of stability, whole body and centroidal angular momentum, and its rate of change.

## II. Materials and Methods

### A. Robot Experiment

*1) Humanoid Robot:* The used robot is RHP Friends [31] (RHP Friends: Robust Humanoid Platform), Kawasaki Robotics, Japan, a humanoid biped robot with 15 segments and 30 degrees of freedom (leg 6 DoF; arm 7 DoF; torso 2 DoF; neck 2 DoF), with a total weight, internal battery included, of 63.85 kg. The robot's height is 1.68 m. The robot has force torque sensors at the ankle and wrist joints.

*2) Gait and Balance Controller:* The RHP Friends used the closed-loop IS-MPC walking controller [32]. The locomotion control scheme uses the extended dynamics of the LIPM to balance walking by relating CoM acceleration to displacement from the ZMP. The system tracks desired velocities and dynamically adjusts the ZMP reference through admittance foot force control to maintain balance. Key components include model-rich closed-loop feedback, which integrates CoM and ZMP measurements from force/torque sensors to predict and adjust for future balance, dynamic replanning to adapt step locations and timings based on real-time disturbances, and feet force control to ensure stable force tracking without oscillations. The control loop was running at 200 Hz.

*3) Experiment Procedures:* The robot was controlled in two locomotion scenarios:

*a) Normal walking with different speeds:* The robot was operated to walk in a straight path across the experiment room at two different speeds: 0.30 $\pm$ 0.02 m/s and 0.15 $\pm$ 0.01 m/s. Four trials were conducted at each speed.

*b) Walking with perturbations:* The robot was controlled to walk over manually placed layer(s) of soft mats. Stepping on the border between the soft mats and the flat ground produced a disturbance. Four levels of perturbations were introduced by increasing the number of soft mats layers from 1 layer, (1.2 $\pm$ 0.04 cm thick), to 4 layers, (4.8 $\pm$ 0.1 cm thick), accordingly. Each perturbation was applied as follows:

1) The robot walked forward at 0.15 m/s.
2) Mats were placed for the robot to step on the edge between the mats and the floor.
3) Immediately after the lift-off, mats were removed.

These steps were repeated after the robot returned to normal gait. Five perturbed steps were performed at each of perturbation levels from 1 to 3. For level 4, four perturbation events that caused falls were performed.

*4) Data processing:* The floating-base kinematics of the robot were estimated with a Lyapunov stable observer [33]. Robot sensors data were sampled at 200 Hz. Given the known relative position of the center of mass (CoM) to the floating base from RHP Friends model, the kinematics provided by the observer enabled the estimation of the CoM trajectory over time. To make the process consistent with human data aquisition, offline $4^{\text{th}}$-order Butterworth low-pass filter was applied at 6 Hz for kinematic data and at 10 Hz for dynamic and force sensor data. From this processed data, the CoM trajectory, dynamic wrenches from force sensors, sensor positions and orientations, feet positions, and centroid dynamics were extracted and used to compute each mechanical descriptor.

### B. Human Experiment

*1) Participants:* Two groups of human participants were recruited for two experiments. For the first group, 4 healthy participants (3 males 1 female, age: 30 $\pm$ 6.5 yr, weight: 65.4 $\pm$ 12.9 kg, height: 172.2 $\pm$ 6.6 cm) were involved in slow walking without perturbation. For the second group, 6 healthy participants (3 males 3 females, age: 37.8 $\pm$ 11.4 yr, weight: 64.7 $\pm$ 12.9 kg, height: 170.3 $\pm$ 6.7 cm) were involved in walking under perturbations experiment. All participants were informed and signed the consent under the ethical agreement number: RCB 2020-A01357-32. None of the participants had a history of locomotion disorders.

*2) Experiment Procedures:* Each participant was instructed to walk on a dual-belt instrumented treadmill with two underlying force plates recording three-dimensional forces and moments at 1,000 Hz. Motion capture was performed throughout the experiment using 50 reflective full-body markers and 9 cameras (MX T20 and Vero, 100 Hz, Vicon Motion Systems Ltd., Oxford, UK). All markers were placed on the participants' skin except for the feet segment, where markers were placed directly on the participants' shoes. Force plate and motion capture data were simultaneously recorded and synchronized on Vicon Nexus software. All participants started with a familiarization phase by walking at 1.2 m/s on the treadmill. Then, recordings were conducted in two scenarios:

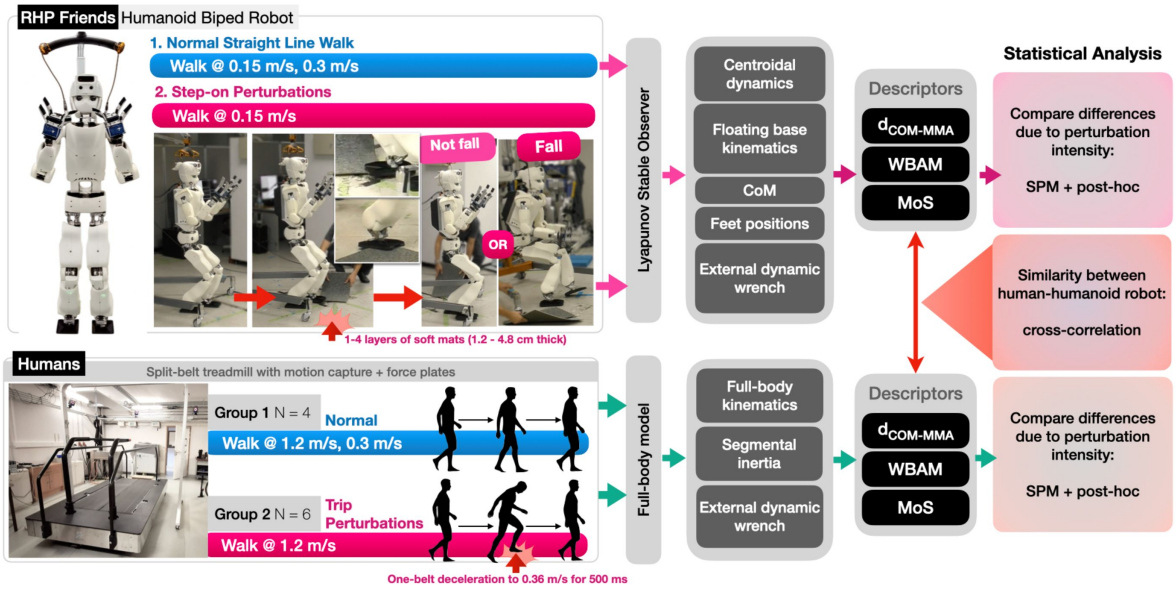


Fig. 1. Overview of materials and methods: experimental setup and data analysis pipeline. Abbreviations: CoM - Center of Mass, $\boldsymbol{d}_{\text{CoM-MMA}}$ - Distance between CoM to the Minimal Moment Axis, WBAM - Whole-Body Angular Momentum, MoS - Margin of Stability, SPM - Spatial Parametric Mapping.

*a) First group:* Participants were instructed to walk at 1.2 m/s for one trial followed by 0.3 m/s for two trials. Each trial consisted of 10-15 gait cycles of normal gait without perturbation. Although the walking speed of 0.3 m/s is much lower than typical physiological gait speeds, it was chosen as a common gait speed for both humans and the RHP Friends, as it represents the robot's maximum stable gait speed. Data collected at this common speed enabled us to compare the patterns and evolution of mechanical descriptors throughout the gait cycle, potentially highlighting scaling factors, and intrinsic behaviors that must be considered for human-robot transferability and interpolation of future results.

*b) Second group:* Participants walked at 1.2 m/s. During that time, they encountered trip perturbations. Extended details of the experiment setup were described in [34]. Side, type and acceleration during the perturbation were randomly determined before the session. Perturbations were triggered via a Lab View interface (National Instruments Corp., Austin, TX, USA) allowing to modify the belt speed at a given instant of the gait cycle. Occurrence was defined at the instant the perturbed foot made contact with the ground. At that point, a target speed signal of $-70\%$ of the initial speed (0.36 m/s) [35] was sent to the treadmill. Acceleration rates were set in the treadmill control software at 3 m/s$^2$. Perturbation duration was set at 500 ms.

*3) Data processing:* Pre-processing was done by applying the same $4^{\text{th}}$-order Butterworth low-pass filter at 6 Hz for motion capture data and at 10 Hz force plates analog data, respectively. Static poses were used to establish a personalized reference full-body model [36], [37]. Kinematics data, including body segment orientation and reconstructed markers' position through time, was acquired using inverse kinematics with rigid body motion constraints. The body CoM position was calculated as the mass-weighted average position of all segment CoM positions. These data are then used to estimate mechanical descriptors of interest.

## C. Computation of mechanical descriptors

*1) Distance between the Center of Mass to the Minimal Moment Axis ($\boldsymbol{d}_{\text{CoM-MMA}}$):* $\boldsymbol{d}_{\text{CoM-MMA}}$ was formulated and calculated as in [19], [2], [20].

$$\boldsymbol{d}_{\text{CoM-MMA}} = \frac{\boldsymbol{F}_{\text{ext}} \times \boldsymbol{M}_{\text{CoM}}}{||\boldsymbol{F}_{\text{ext}}||^2} \tag{1}$$

where $\boldsymbol{F}_{\text{ext}}$ is the resultant force, and $\boldsymbol{M}_{\text{CoM}}$ is the resultant moment expressed at the body's center of mass (CoM).

*2) Whole-Body Angular Momentum ($\boldsymbol{L}_{WB}$ or WBAM):* For the robot, the WBAM was equivalent to the centroid angular momentum given by the state estimator and encoders. For humans, it was calculated using the following formula:

$$\boldsymbol{L}_{\text{WB}} = \sum_{i=1}^{i=N} \frac{[\boldsymbol{I}_i\boldsymbol{\omega}_i + (\boldsymbol{p}_i - \boldsymbol{p}_{\text{CoM}}) \times m_i(\boldsymbol{v}_i - \boldsymbol{v}_{\text{CoM}})]}{M \cdot V \cdot H} \tag{2}$$

where $p_i$ , $p_{\text{CoM}}$, $v_i$ , $v_{\text{CoM}}$ are the position and velocity vectors at the center of mass (CoM) of the $i^{\text{th}}$ segment and the body respectively, $m_i$, $I_i$, $\omega_i$ are the segment mass, their matrix of inertia and their angular velocity respectively. WBAM was normalized by $(M \cdot V \cdot H)$ of their respective subjects where $M$ is the total participant's or the robot's mass in $kg$, $V$ is the average gait speed of the respective gait cycle, and $H$ is the total height of each participant or the robot. Time rate of change of the WBAM was also computed as $\dot{\boldsymbol{L}}_{\text{WB}} = d\boldsymbol{L}_{\text{WB}}/dt$.

*3) Margin of Stability (MoS):* It is defined as the distance from the extrapolated center of mass (XCoM) to the nearest edge of the base of support (BoS).

$$b = \pm \min(||\boldsymbol{p}_{\in \text{BoS}} - \boldsymbol{p}_{\text{XCoM}}||) \tag{3}$$

where $\boldsymbol{p}_{\text{XCoM}}$ was calculated as equal to $\boldsymbol{p}_{\text{CoM}} + \boldsymbol{v}_{\text{CoM}}\sqrt{l/g}$. $\boldsymbol{p}_{\text{CoM}}$ is the vector position of the CoM respectively, $l$ is the vertical height of the CoM position and $g$ is the gravitational acceleration. A sign convention is used for $b$. A positive MoS indicates that XCoM is within the BoS. Conversely, a negative MoS means the XCoM is outside the BoS. The BOS was represented by the set of hull points of all foot vertices in contact with the ground. For RHP-Friends, four corner vertices of each foot were used. For humans, all four markers on each foot segment were used.

### D. Statistical Analysis

Normallity and homogeneity of variances was assessed with Kolmogorov-Smirnov and Levene's tests to determine appropriate statistical tests for comparative analyses. In order to confront biped robot and humans normal walking without perturbations, comparative analysis was done for $\boldsymbol{d}_{\text{CoM-MMA}}$. Four data groups were selected for the analysis, including human (first group experiment) walking without perturbation at 1.2 m/s and 0.3 m/s, RHP Friends walking at 0.3 m/s and 0.15 m/s. In order to quantify the performance of the different mechanical descriptors during walking under perturbations, four comparative analyses were performed on all four mechanical descriptors. Seven groups of data were selected, including human (second group experiment) normal and perturbed walking at 1.2 m/s and all four levels of RHP Friends perturbed walking and normal walking at 0.15 m/s.

For each comparative analysis, the input data was arranged as two matrices, $\boldsymbol{M}$ and $\boldsymbol{A}$. $\boldsymbol{M}$ is a matrix having each column containing a time series of a selected descriptor value for each gait cycle. This input matrix has a size of $Y \times N$ where $Y$ is the resolution of the gait cycle(s), and $N$ is the number of different gait cycles. While Matrix $\boldsymbol{A}$ contains group labels, size $1 \times N$. Then, the input data was used for Spatial Parametric Mapping (SPM) using two-tailed one-way ANOVA (or Levene's test for non-parametric data), followed by post-hoc analysis using two-tailed t-test, paired when comparing the same participants and unpaired when comparing humans and robots, (or Wilcoxon Signed Rank test for non-parametric data) on all possible pairs with corrected Bonferroni alpha level. All statistical tests had the null hypothesis, as no significant difference existed between the groups or the pairs. Initial alpha levels were set at 0.05. To distinguish whether significant differences in descriptor values were from gait variability or the induced perturbations, cross-comparisons were conducted during the post-hoc analysis. This result was taken into account for the statistical interpretations to ensure that the observed effects were primarily attributable to the perturbations rather than inherent subject variability. Statistics were performed on MATLAB 2023b using custom code, Statistics and Machine Learning Toolbox, and spm1d package.

## III. Results & Discussion

### A. Normal gait profile in humans and biped robot

As shown in Fig. 1, humans and RHP Friends were subjected to similar range of external actions during baseline walking, despite the robot exhibited more jerk and bounce at ground contact due to its non-compliance feet. During baseline walking, humans at 0.3 m/s and RHP Friends, at 0.3 m/s and 0.15 m/s, demonstrated similar %double and %stance with respect to their gait cycle duration at $34.81 - 37.29 \pm 2.73 - 3.98\%$ and $65.80 - 68.76 \pm 1.43 - 2.88\%$ for %double stance phase and %stance, respectively. When walking at normal speed (1.2 m/s), humans showed $23.73 \pm 1.89\%$ of double stance and $62.25 \pm 1.06\%$ for stance phase. At 0.3 m/s, the the robot showed the gait cycle duration of $2.22 \pm 0.02$ s and step lengths of $33.64 \pm 2.28$ cm. Humans showed shorter gait cycle duration and step length with higher degree of standard deviations ($2.05 \pm 0.14$ s for gait cycle duration, and for $34.77 \pm 5.86$ cm step lengths). At higher gait speeds, humans and RHPS Friends use different strategies. RHPS Friends increased step length to to $56.34 \pm 5.24$ cm, at gait speed 0.3 m/s, with a constant gait cycle duration. In contrast, humans achieved 1.2 m/s using both shorter gait cycles ($1.08 \pm 0.02$ s) and longer steps ($62.45 \pm 2.64$ cm).

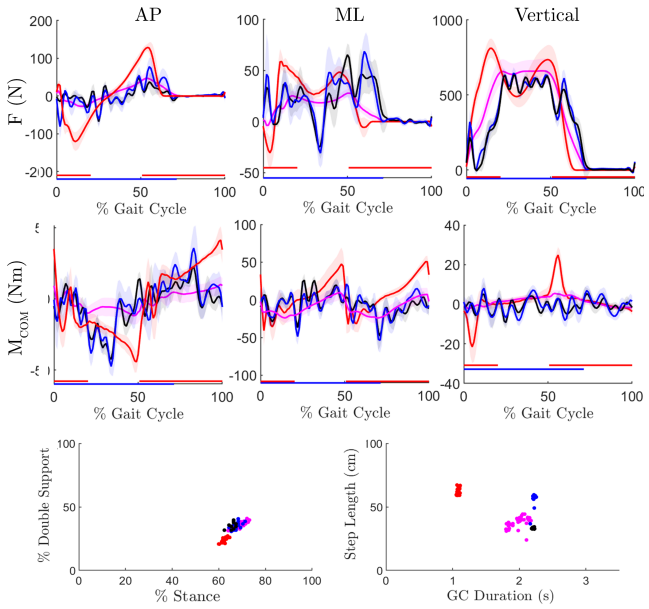


Fig. 2. Gait characteristics during normal walking showing three dimensional external force (N) and moment at the CoM (Nm), and gait profile including % double stance vs % stance, step length (cm) vs gait cycle duration (s). Color legends: — human 1.2 m/s, — human 0.3 m/s, — RHP Friends 0.3 m/s, — RHP Friends 0.15 m/s; Gait cycle (horizontal bars): stance phase of — dominant side, — non-dominant side.

### B. Behavior of $\boldsymbol{d}_{\text{CoM-MMA}}$ during normal walking

The behavior of the $\boldsymbol{d}_{\text{CoM-MMA}}$ during baseline walking in humans and RHP Friends are shown in Fig. 2. In humans, when walking at normal speed of 1.2 m/s, the average size of $\boldsymbol{d}_{\text{CoM-MMA}}$ was $3.81 \pm 1.30$ cm. $\boldsymbol{d}_{\text{CoM-MMA}}$ amplitudes had an increasing trend and reached a maximum during the single stance phase. The pattern was slightly shifted forward when walked at slow speed, while the range of amplitudes was also decreased ($2.71 \pm 0.39$ cm). For RHP Friends, the average

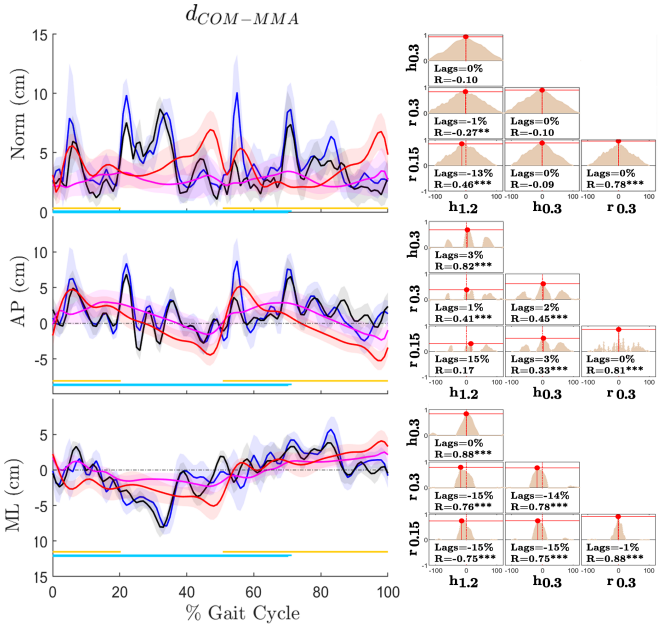


Fig. 3. Left) The distance between the center of mass to the minimal moment axis in (cm) expressed in pelvis frame (humans) or floating base frame (RHP Friends): norms, AP component, and ML component. Color legends: — human 1.2 m/s, — human 0.3 m/s, — RHP Friends 0.3 m/s, — RHP Friends 0.15 m/s, stance phase of — dominant side, — non-dominant side. Right) Cross-correlation matrix showing correlation coefficient with respect to time lags. The maximum correlation and the time lag value which it occured were shown as text. Abbreviations: $h_{1.2}$ - human 1.2 m/s, $h_{0.3}$ - human 0.3 m/s, $r_{0.3}$ - robot 0.3 m/s, $r_{0.15}$ - robot 0.15 m/s.

sizes of $\boldsymbol{d}_{\text{CoM-MMA}}$ were at $4.22\pm1.99$ cm and $3.51\pm1.78$ cm for 0.3 m/s and 0.15 m/s walk, respectively. Each component average value can be found on TABLE I.

TABLE I

AVERAGE LENGTH OF $\boldsymbol{d}_{\text{CoM-MMA}}$ DURING BASELINE WALKING

| Group - Speed | Norm (cm) | AP (cm) | ML (cm) |
|---|---|---|---|
| Human @1.2 m/s | $3.81 \pm 1.30$ | $2.54 \pm 1.24$ | $2.43 \pm 1.07$ |
| Human @0.3 m/s | $2.71 \pm 0.39$ | $2.02 \pm 0.51$ | $1.37 \pm 0.44$ |
| RHP Friends @0.3 m/s | $4.22 \pm 1.99$ | $2.62 \pm 1.73$ | $2.74 \pm 1.45$ |
| RHP Friends @0.15 m/s | $3.51 \pm 1.78$ | $2.10 \pm 1.37$ | $2.40 \pm 1.55$ |

In Fig. 2, cross-correlation analysis revealed significant ($p < 0.001$) and strong internal correlations ($R = 0.78 - 0.88$), with in-phase evolution (0–1% lags), in the distances observed among RHP Friends across total size, antero-posterior (AP), and medio-lateral (ML) components. For humans, similar correlations were only found in AP (3% lags, $R = 0.82$, $p < 0.001$) and ML components (0% lags, $R = 0.88$, p<0.001), but not the norms. In terms of correlation between humans and RHP Friends, there were significant ($p < 0.001$) and with varying degree of correlation ($R = 0.33 - 0.78$) in both AP and ML components; however, these relationships were absent for the norm. The timing of patterns in humans were shifted forwarded in %gait cycles compared to RHP Friends as suggested by the %lags of 13 to 15% from the cross-correlation analysis. The SPM ANOVA and pair-wise post-hoc analysis, showed multiple small clusters (1 to 7% of the gait cycle) of significant differences between human and RHP Friends, including all possible human-robot pairs, scattered throughout the cycle. These small clusters were not relevant to gait cycle events or phases. These differences signify that the waveform shape of $\boldsymbol{d}_{\text{CoM-MMA}}$ in RHP Friends and humans were not homogeneous, confirming the observation that, despite in-phase trends of changes throughout the gait cycle, $\boldsymbol{d}_{\text{CoM-MMA}}$ in RHP Friends showed a more noisy behavior. These differences in $\boldsymbol{d}_{\text{CoM-MMA}}$ observed between humans and biped robots may be attributed to the dynamic control of the gait. As shown in Fig. 1, humans and RHP Friends exhibit distinct patterns in the net external moment expressed at CoM. Humans typically show smoother and more consistent changes in this moment, reflecting their natural ability to adapt and maintain stability during walking. In contrast, RHP Friends demonstrates a more abrupt and noisy pattern, likely due to differences in mechanical properties and controls of the biped robot compared to human musculoskeletal dynamics.

### C. Behavior of $\boldsymbol{d}_{\text{CoM-MMA}}$ under perturbations

In Fig. 3, the $\boldsymbol{d}_{\text{CoM-MMA}}$ were converted to dimensionless form by dividing by the robot's/subjects' respective heights. Regardless, upon analysis with original unit, not shown here, the same final statistical conclusions were reached. During the perturbed stance phase, the norm of the $\boldsymbol{d}_{\text{CoM-MMA}}$ were consistently increased in both RHP Friends and humans. Consistent fluctuations were observed in both the AP and ML components. Mean $\boldsymbol{d}_{\text{CoM-MMA}}$ curves at each perturbation level suggested a positive correlation between perturbation intensity and the magnitude of $\boldsymbol{d}_{\text{CoM-MMA}}$ fluctuations (Table II). In trials not leading to a fall, all $\boldsymbol{d}_{\text{CoM-MMA}}$ components returned to their baseline values within the following gait cycle. In contrast, during falls, the three dimentional distance continued to exponentially increase as the fall progressed.

The results from SPM ANOVA and post-hoc pair-wise t-tests revealed significant differences in the total size of $\boldsymbol{d}_{\text{CoM-MMA}}$ between fall and all non-fall gait cycles, and in the AP component between fall and non-fall cycles under the level 3 perturbations. These differences were obvious for the gait cycle following the perturbed cycle. Other significant clusters were small and did not contain meaningful interpretation regarding either the perturbations or falls. The cross-correlation studies shows that the evolution pattern under perturbations of human and robot were correlated ($R = 0.25 - 0.45$ for the norms, $R = 0.34 - 0.46$ for AP component, and $R = 0.65 - 0.69$ for the ML component) regardless of the levels and methods of the perturbations. This result suggests that, despite differences in the perturbation methods (trip v.s. step-over) and agents' dynamics (humans v.s. biped robot), similar patterns of evolution of $\boldsymbol{d}_{\text{CoM-MMA}}$ emerged. For the negative statistical results at % gait cycles where the mean curves of $\boldsymbol{d}_{\text{CoM-MMA}}$ seemed to be different among different levels of perturbations and agents, they can be explained by the large degree of standard deviations which decreased the level of statistical power and confidence, especially with limited amount of samples.

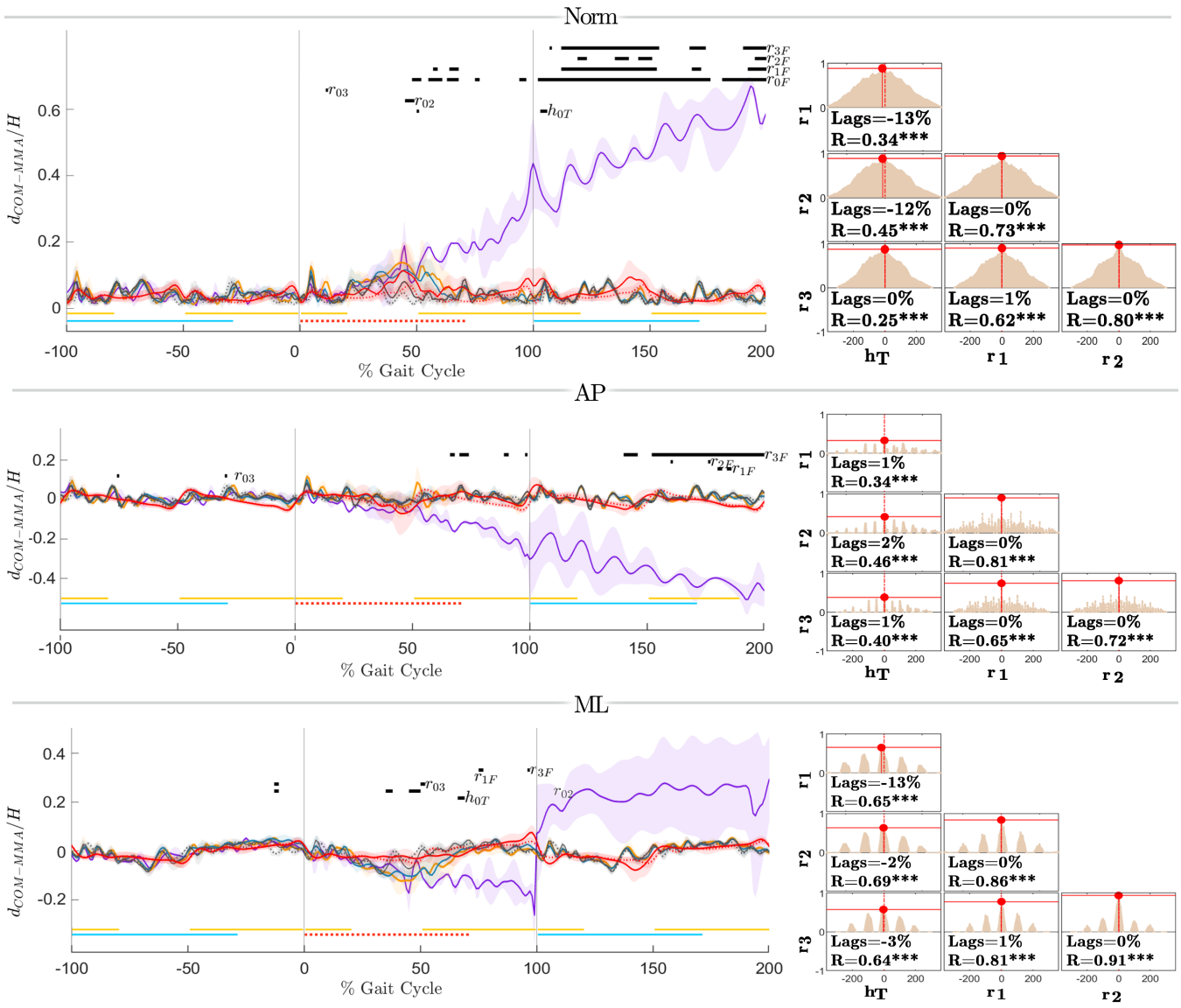


Fig. 4. Left) The distance between the center of mass to the minimal moment axis during walking under different levels of perturbations : norms, AP component, and ML component. Color legends: RHP Friends --- without perturbation, with perturbations — level 1, — level 2, — level 3, — level 4; Humans --- without perturbation, — with trip perturbations; Gait cycle: stance phase of — dominant side, — non-dominant side, and --- perturbed stance; Statistics: — indicating regions of %gait cycle with significant differences of $\boldsymbol{d}_{\text{CoM-MMA}}$. Right) Cross-correlation matrix showing correlation coefficient with respect to time lags. The maximum correlation and the time lag value which it occurred were shown as text. Abbreviations: $h_0$ - human without perturbation, $h_T$ - human trip trials (no fall), $r_0$ - RHP Friends without perturbation, $r_{1-3}$ - under perturbation levels 1-3 (no fall), $r_F$ - fall trials.

TABLE II

AVERAGE LENGTH OF $\boldsymbol{d}_{\text{CoM-MMA}}$ (CM) DURING PERTURBED WALKING

| Group | Norm | | | AP component | | | ML component | | |
|---|---|---|---|---|---|---|---|---|---|
| | Pre | Event | Post | Pre | Event | Post | Pre | Event | Post |
| $H_0$ | $3.80 \pm 0.62$ | $3.80 \pm 0.66$ | $3.83 \pm 0.73$ | $2.55 \pm 0.41$ | $2.52 \pm 0.39$ | $2.56 \pm 0.47$ | $2.41 \pm 0.79$ | $2.43 \pm 0.81$ | $2.45 \pm 0.79$ |
| $H_T$ | $3.83 \pm 0.73$ | $5.50 \pm 1.41^*$ | $4.67 \pm 1.32$ | $2.56 \pm 0.47$ | $4.06 \pm 1.20^*$ | $3.06 \pm 1.02$ | $2.45 \pm 0.79$ | $2.91 \pm 1.06^*$ | $3.03 \pm 1.21$ |
| $R_0$ | $3.52 \pm 0.08$ | $3.53 \pm 0.07$ | $3.53 \pm 0.07$ | $2.14 \pm 0.16$ | $2.12 \pm 0.19$ | $2.08 \pm 0.16$ | $2.40 \pm 0.13$ | $2.41 \pm 0.14$ | $2.43 \pm 0.12$ |
| $R_1$ | $4.32 \pm 0.59$ | $4.44 \pm 0.52$ | $3.99 \pm 0.26$ | $2.36 \pm 0.26$ | $2.45 \pm 0.29$ | $2.31 \pm 0.16$ | $3.07 \pm 0.57$ | $3.17 \pm 0.64$ | $2.80 \pm 0.25$ |
| $R_2$ | $4.11 \pm 0.34$ | $5.93 \pm 0.95^*$ | $3.70 \pm 0.11$ | $2.16 \pm 0.11$ | $3.04 \pm 0.60^*$ | $2.26 \pm 0.07$ | $3.04 \pm 0.42$ | $4.49 \pm 0.91^*$ | $2.47 \pm 0.16$ |
| $R_3$ | $4.01 \pm 0.38$ | $6.56 \pm 1.45^*$ | $3.94 \pm 0.32$ | $2.39 \pm 0.07$ | $3.58 \pm 0.74^*$ | $2.30 \pm 0.15$ | $2.72 \pm 0.44$ | $4.60 \pm 1.60^*$ | $2.73 \pm 0.54$ |
| $R_F$ | $3.88 \pm 0.32$ | $13.73 \pm 3.57^*$ | $48.23 \pm 2.82^*$ | $2.43 \pm 0.30$ | $9.01 \pm 1.68^*$ | $35.40 \pm 12.20^*$ | $2.58 \pm 0.07$ | $9.41 \pm 3.08^*$ | $23.61 \pm 21.68^*$ |

Legends - Pre: normal gait cycles, Event: perturbed gait cycles, Post: post-perturbation gait cycles, $H_0$: Human baseline at 1.2 m/s. $H_T$: human trip at 1.2 m/s, $R_0$: robot baseline at 0.15 m/s, $R_1 - R_3$: robot under perturbation levels 1-3, $R_F$: robot with falls; *: significant differences from normal cycles.

### D. Other descriptors

Figure 4 shows the behavior of the WBAM norms, its time rate of change, and the MoS norms during normal and perturbed walking. Consistent with prior studies [38], the baseline patterns of MoS reached a maximum during early double support, and decreased to a minimum at the end of single support phase. For both humans and RHP Friends, perturbations decreased the norm of MoS during

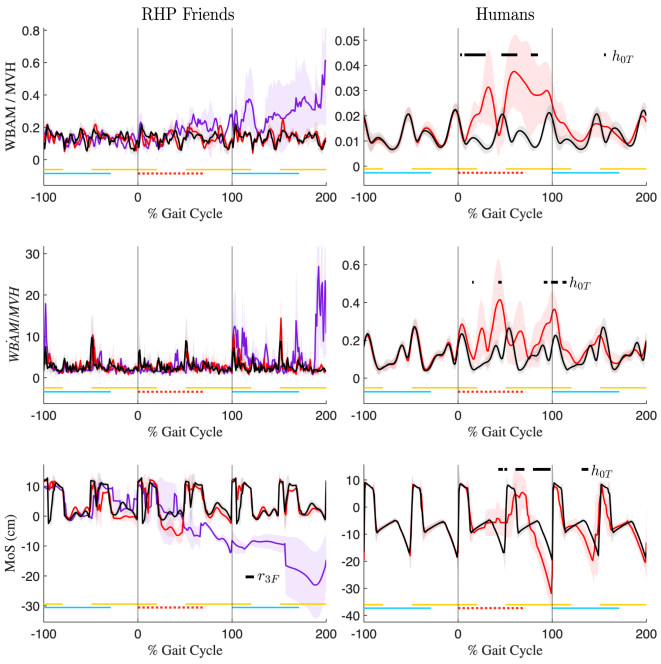


Fig. 5. Behavior of other descriptors during normal walking (baseline) and under perturbations, including: normalized WBAM, the rate of change of normalized WBAM, and the margin of stability (MoS). Left) RHP Friends, Right) Humans. Color legends: — baseline, with perturbations — non-falls, — falls; Gait cycle: stance phase of — dominant side, — non-dominant side, and --- perturbed stance; Statistics: — indicating regions of %gait cycle with significant differences. Abbreviations: $h_0$ - Human baseline, $h_T$ - trip trials; $r_0$ - robot baseline, $r_n$ - perturbed trials (not fall), $r_F$ - fall trials.

the swing phase of perturbed leg. In non-fall trials, the MoS recovered to normal with a gait cycle, while it remained lower during falls, as observed in [39]. For WBAM, there were significant increases under perturbation in humans from mid-stance through the swing phase, similar to [40], whereas the robot only showed increases during the pre-swing and swing phases. The time rate of change of WBAM in humans showed a large positive change during the stance of perturbed cycle, however, this pattern was not visible in the robot. The observed increases in humans during trips were likely due to forward rotation of the upper body under initial imbalance as previously demonstrated in [41]. The differences in descriptor behaviors between humans and the robot are expected as the dynamics, control strategies, and perturbation methods were different. Regardless, these findings highlight that these descriptors are highly sensitive to many gait variability factors. While all metrics demonstrated observable differences in the degree of fluctuations depending on the level of perturbations, they were less obvious, and lacked clear coherent patterns of fluctuation even under the same perturbation method. Only fall trials in the robot showed clear differences in descriptors' value with respect to non-fall trials; however, these differences were at the post perturbation gait cycle and were not observable during perturbed stances. This suggests that these descriptors might have limited capability to detect an imminent fall early. According to SPM ANOVA and post-hoc analysis, WBAM and MoS showed meaningful significant differences between the baseline and under trip condition in humans. In the robot, despite visible differences in mean curves, large variability among trials resulted in only small, scattered clusters of differences across all descriptors and were not significant enough to represent perturbation events or falls.

### *E. Considerations, Limitations & Future Research*

Scaling by height or CoM height can standardize stability measurements across different subjects, but it does not account for variations in body mass distribution and joint configurations, especially between humans and robots. Normalizing by dynamic gait parameters (e.g., characteristic length) instead of static height may be more robust, as these are directly linked to locomotion dynamics and could enhance a descriptor's sensitivity to stability changes.

In this study, normalizing $\boldsymbol{d}_{\text{CoM-MMA}}$ by height did not significantly affect the results, likely because the robot and human subjects had similar height ranges and CoM positions. However, since stability is more closely linked to gait dynamics (e.g., speed, step frequency, and CoM velocity), normalizing descriptors with such dynamic parameters could provide a more accurate stability assessment.

One limitation of our experiment was the safety lifter needed to protect the robot during falls. To avoid entanglement with the lifter's ropes, we used manually placed soft mats for perturbations instead of fixed obstacles. While this introduced variability, it allowed us to test our stability criterion across a broader range of scenarios, such as stepping on a mat's edge, thereby testing the generality of our findings.

Future research should investigate how different fall types, timings, and recovery strategies affect stability. Exploring varied perturbations (e.g., lateral pushes) is crucial for understanding fall dynamics and the differences in human versus robot recovery. These insights can inform the design of more effective fall prevention systems, advanced robots, and exoskeletons.

## IV. CONCLUSIONS

This study validates the stability metric $\boldsymbol{d}_{\text{CoM-MMA}}$ for both humans and biped robots, showing that it is predictive of the instability level and fall. Due to their similarity in observed behaviors, $\boldsymbol{d}_{\text{CoM-MMA}}$ shows promise as a universal descriptor for stability. Future work should investigate the metric integration into advanced robotic and clinical systems, e.g., exoskeleton control and fall detection devices, to enhance safety and mobility for both humans and robots.

## REFERENCES

[1] Sjoerd M Bruijn, OG Meijer, PJ Beek, and Jaap H van Dieen. Assessing the stability of human locomotion: a review of current measures. *Journal of the Royal Society Interface*, 10(83):20120999, 2013.

[2] François Bailly, Justin Carpentier, Bertr Pinet, Philippe Souères, and Bruno Watier. A mechanical descriptor of human locomotion and its application to multi-contact walking in humanoids. In *2018 7th IEEE International Conference on Biomedical Robotics and Biomechatronics (Biorob)*, pages 350–356. IEEE, 2018.

[3] Shuuji Kajita, Fumio Kanehiro, Kenji Kaneko, Kazuhito Yokoi, and Hirohisa Hirukawa. The 3d linear inverted pendulum mode: A simple modeling for a biped walking pattern generation. In *Proceedings 2001 IEEE/RSJ International Conference on Intelligent Robots and Systems. Expanding the Societal Role of Robotics in the the Next Millennium (Cat. No. 01CH37180)*, volume 1, pages 239–246. IEEE, 2001.

[4] Miomir Vukobratović and Jurij Stepanenko. Mathematical models of general anthropomorphic systems. *Mathematical biosciences*, 17(3-4):191–242, 1973.

[5] Shuuji Kajita, Fumio Kanehiro, Kenji Kaneko, Kiyoshi Fujiwara, Kensuke Harada, Kazuhito Yokoi, and Hirohisa Hirukawa. Biped walking pattern generation by using preview control of zero-moment point. In *2003 IEEE international conference on robotics and automation (Cat. No. 03CH37422)*, volume 2, pages 1620–1626. IEEE, 2003.

[6] Pierre-Brice Wieber. Trajectory free linear model predictive control for stable walking in the presence of strong perturbations. In *2006 6th IEEE-RAS International Conference on Humanoid Robots*, pages 137–142. IEEE, 2006.

[7] Toru Takenaka, Takashi Matsumoto, and Takahide Yoshiike. Real time motion generation and control for biped robot: 1st report: walking gait pattern generation. In *Proceedings of the 2009 IEEE/RSJ International Conference on Intelligent Robots and Systems*, IROS'09, page 1084–1091. IEEE Press, 2009.

[8] Johannes Englsberger, Christian Ott, and Alin Albu-Schäffer. Three-dimensional bipedal walking control based on divergent component of motion. *IEEE Transactions on Robotics*, 31(2):355–368, 2015.

[9] Jerry Pratt, John Carff, Sergey Drakunov, and Ambarish Goswami. Capture point: A step toward humanoid push recovery. In *2006 6th IEEE-RAS International Conference on Humanoid Robots*, pages 200–207, 2006.

[10] Tomomichi Sugihara and Mitsuharu Morisawa. A survey: dynamics of humanoid robots. *Advanced Robotics*, 34(21-22):1338–1352, 2020.

[11] At L Hof, MGJ Gazendam, and WE Sinke. The condition for dynamic stability. *Journal of biomechanics*, 38(1):1–8, 2005.

[12] Stéphane Caron. Biped stabilization by linear feedback of the variable-height inverted pendulum model. In *2020 IEEE International Conference on Robotics and Automation (ICRA)*, pages 9782–9788. IEEE, 2020.

[13] Marko B Popovic, Ambarish Goswami, and Hugh Herr. Ground reference points in legged locomotion: Definitions, biological trajectories and control implications. *The international journal of robotics research*, 24(12):1013–1032, 2005.

[14] Yukai Gong and Jessy W Grizzle. Zero dynamics, pendulum models, and angular momentum in feedback control of bipedal locomotion. *Journal of Dynamic Systems, Measurement, and Control*, 144(12):121006, 2022.

[15] Hugh Herr and Marko Popovic. Angular momentum in human walking. *Journal of experimental biology*, 211(4):467–481, 2008.

[16] Kyle H Yeates, Ava D Segal, Richard R Neptune, and Glenn K Klute. Balance and recovery on coronally-uneven and unpredictable terrain. *Journal of biomechanics*, 49(13):2734–2740, 2016.

[17] Jennifer K Leestma, Pawel R Golyski, Courtney R Smith, Gregory S Sawicki, and Aaron J Young. Linking whole-body angular momentum and step placement during perturbed human walking. *Journal of Experimental Biology*, 226(6):jeb244760, 2023.

[18] Teddy Caderby, Angélique Lesport, Nicolas A Turpin, Georges Dalleau, Bruno Watier, Thomas Robert, Nicolas Peyrot, and Jérémie Begue. Influence of aging on the control of the whole-body angular momentum during volitional stepping: An ucm-based analysis. *Experimental Gerontology*, 178:112217, 2023.

[19] Justin Carpentier, Mehdi Benallegue, Nicolas Mansard, and Jean-Paul Laumond. Center-of-mass estimation for a polyarticulated system in contact—a spectral approach. *IEEE Transactions on Robotics*, 32(4):810–822, 2016.

[20] Nahime Al Abiad, Helene Pillet, and Bruno Watier. A mechanical descriptor of instability in human locomotion: experimental findings in control subjects and people with transfemoral amputation. *Applied Sciences*, 10(3):840, 2020.

[21] Bruno Watier, Jérémie Begue, Hélène Pillet, and Teddy Caderby. Instability during stepping and distance between the center of mass and the minimal moment axis: Effect of age and speed. *Applied Sciences*, 13(19):10574, 2023.

[22] Jonathan B. Dingwell and Hyun Gu Kang. Differences between local and orbital dynamic stability during human walking. *Journal of Biomechanical Engineering*, 129(4):586–593, 12 2006.

[23] Marcel JP Toebes, Marco JM Hoozemans, Regula Furrer, Joost Dekker, and Jaap H van Dieën. Local dynamic stability and variability of gait are associated with fall history in elderly subjects. *Gait & posture*, 36(3):527–531, 2012.

[24] Laura Hak, Han Houdijk, Frans Steenbrink, Agali Mert, Peter van der Wurff, Peter J Beek, and Jaap H van Dieën. Speeding up or slowing down?: Gait adaptations to preserve gait stability in response to balance perturbations. *Gait & posture*, 36(2):260–264, 2012.

[25] Jooeun Ahn and Neville Hogan. Is estimation of floquet multipliers of human walking valid? In *2014 40th Annual Northeast Bioengineering Conference (NEBEC)*, pages 1–2, 2014.

[26] Daniel Williams and Anne E Martin. Predicting fall risk using multiple mechanics-based metrics for a planar biped model. *PLoS one*, 18(3):e0283466, 2023.

[27] Richard P. Boland, Tobias Galla, and Alan J. McKane. Limit cycles, complex floquet multipliers, and intrinsic noise. *Phys. Rev. E*, 79:051131, May 2009.

[28] Antonis Ekizos, Alessandro Santuz, Arno Schroll, and Adamantios Arampatzis. The maximum lyapunov exponent during walking and running: Reliability assessment of different marker-sets. *Frontiers in Physiology*, 9, 2018.

[29] Arian Vistamehr, Steven A Kautz, Mark G Bowden, and Richard R Neptune. Correlations between measures of dynamic balance in individuals with post-stroke hemiparesis. *Journal of biomechanics*, 49(3):396–400, 2016.

[30] Richard R Neptune and Arian Vistamehr. Dynamic balance during human movement: measurement and control mechanisms. *Journal of Biomechanical Engineering*, 141(7):070801, 2019.

[31] Mehdi Benallegue, Guillaume Lorthioir, Antonin Dallard, Rafael Cisneros-Limón, Iori Kumagai, Mitsuharu Morisawa, Hiroshi Kaminaga, Masaki Murooka, Antoine André, Pierre Gergondet, Kenji Kaneko, Guillaume Caron, Fumio Kanehiro, Abderrahmane Kheddar, Soh Yukizaki, Junichi Murakami, Junichi Karasuyama, and Masayuki Kamon. Humanoid Robot RHP Friends: Seamless Combination of Autonomous and Teleoperated Tasks in a Nursing Context. *IEEE Robotics and Automation Magazine*, pages 2–12, January 2025.

[32] Antonin Dallard, Mehdi Benallegue, Nicola Scianca, Fumio Kanehiro, and Abderrahmane Kheddar. Robust bipedal walking with closed-loop mpc: Adios stabilizers. *Submitted to IEEE Transactions on Robotics*, 2024.

[33] Mehdi Benallegue, Rafael Cisneros, Abdelaziz Benallegue, Yacine Chitour, Mitsuharu Morisawa, and Fumio Kanehiro. Lyapunov-stable orientation estimator for humanoid robots. *IEEE Robotics and Automation Letters*, 5(4):6371–6378, 2020.

[34] Ariane Lallès, Bruno Watier, and Hélène Pillet. Dynamic Criterion to Quantify Instability During Locomotion. *2024 International Symposium on 3D Analysis of Human Movement (3DAHM)*, pages 1–5, December 2024.

[35] Rebecca Macaluso, Kyle Embry, Dario J. Villarreal, and Robert D. Gregg. Parameterizing human locomotion across quasi-random treadmill perturbations and inclines. *IEEE Transactions on Neural Systems and Rehabilitation Engineering*, 29:508–516, 2021.

[36] Raphaël Dumas, Laurence Cheze, and J-P Verriest. Adjustments to mcconville et al. and young et al. body segment inertial parameters. *Journal of biomechanics*, 40(3):543–553, 2007.

[37] Hélène Pillet, Xavier Drevelle, Xavier Bonnet, Coralie Villa, Noël Martinet, Christophe Sauret, Joseph Bascou, Isabelle Loiret, Francis Djian, Nathalie Rapin, et al. Apsic: Training and fitting amputees during situations of daily living. *IRBM*, 35(2):60–65, 2014.

[38] Carolin Curtze, Tom JW Buurke, and Christopher McCrum. Notes on the margin of stability. *Journal of biomechanics*, 166:112045, 2024.

[39] RJ Boekesteijn, NLW Keijsers, K Defoort, ACH Geurts, and K Smulders. Individuals with knee osteoarthritis show few limitations in balance recovery responses after moderate gait perturbations. *Clinical Biomechanics*, 114:106218, 2024.

[40] Shabnam Shokouhi, Hossein Mokhtarzadeh, and Peter Vee-Sin Lee. Lower extremity joint power and work during recovery following trip-induced perturbations. *Gait & Posture*, 107:1–7, 2024.

[41] Mirjam Pijnappels, Maarten F Bobbert, and Jaap H van Dieën. Contribution of the support limb in control of angular momentum after tripping. *Journal of biomechanics*, 37(12):1811–1818, 2004.